

A COMPARATIVE STUDY FOR CHOOSING THE BEST KINETIC MODEL USING DIFFERENT ERROR METRICS

Ajay Kumar Agarwal

Department of Mining Engineering
Visvesvaraya National Institute of Technology,
Nagpur 440010, India
akagarwal@mng.vnit.ac.in

Received 23 August 2024
Accepted 17 January 2025

DOI: 10.59957/jctm.v60.i3.2025.4

ABSTRACT

In the present investigations, a comparison of fly ash and cow dung ash was carried out to study the adsorption kinetics of Nickel ions present in aqueous solution. Various kinetic models are evaluated during these investigations, which include pseudo-first-order, pseudo-second-order, intra-particle diffusion, fractional power, and Elovich models. These models were exhaustively evaluated and compared using eighteen different error functions. An overall performance indicator metric has also been discussed that helps in ranking the different kinetic models for estimation of adsorption capacity (q) based on the values of different error functions. After analysing these results, it was observed that the kinetic models can be ranked from best to worst with respect to q , determination for cow dung ash and are as follows: pseudo-first order, pseudo-second order, Intra-particle diffusion, Elovich, and Fractional power. Similarly, for fly ash adsorbent, the ranking of kinetic models from best to worst was found to be: pseudo-second-order, intra-diffusion particle, fractional power, Elovich, and pseudo-first-order.

Keywords: adsorption, error metrics, kinetics, overall performance indicator.

INTRODUCTION

Heavy metal ions present in industrial effluents are a source of hazardous pollutants [1]. Increased industrial and human activities are the main reasons for the higher level of metal ions present in wastewater [2, 3]. Effluents consisting of nickel ions have a significant concern when discharged into the water bodies. Once released into the environment, nickel ions accumulate in living tissues via the food chain and cause toxicity even at lower concentrations. The various literature available indicates that its toxicity depends on the dose, time of exposure, and individual susceptibility [4, 5]. Due to its toxic properties, the removal of nickel ions from the contaminated water has drawn the attention of researchers across the world. Chemical precipitation, ion exchange, flotation, biological treatment, and adsorption are often used to remove heavy metals from

wastewater [6]. Amongst several different removal techniques, adsorption is known for its economics and usefulness. Therefore, in the present investigations, two low-cost adsorbents namely fly ash (FA) and cow dung ash (CDA) were used to adsorb the nickel ions present in the water. To design an adsorption process, it is very important to study the kinetic aspects of the same. With a clear understanding of the kinetic behaviour, one can effectively determine the optimal contact time between the sorbent and sorbate, ensuring proper interpretation of experimental data [7, 8].

For studying the kinetic behaviours of FA and CDA as an adsorbent, five different kinetic models were used. These mathematical kinetic models are used for the correct interpretation of experimental adsorption results.

However, the main challenge is determining which kinetic model should be selected for describing the kinetic process of adsorption most accurately. In

this regard, this paper has contributed an extensive evaluation for comparing and analysing the performance of different kinetic models by using eighteen different error functions. It was found that there is no single kinetic model that outperforms the other models with respect to all the error functions discussed. Thus, in this regard, this paper has also proposed an Overall Performance Indicator metric that helps to select the best performing kinetic model using the values obtained for the error functions by the kinetic models.

EXPERIMENTAL

The batch experiments were conducted to study the kinetic behavior of nickel ions for adsorption on FA and CDA. To carry out these batch experiments, the aqueous solution containing 20 mg L⁻¹ of Ni ions concentration was prepared. All the batch experiments were conducted under constant stirring conditions at an RPM of 150. During the experimentation, the dose of adsorbent i.e. fly ash and cow dung ash was maintained as 10 g per 100 mL and 1 g per 100 mL respectively. The pH of the aqueous solution was measured as 7.3. After each experiment, the adsorbent was separated from the solution, and the remaining solution was used to measure the concentration of nickel ions.

Equipment and chemicals

In the laboratory, aqueous solutions of Ni²⁺ ions of different known concentrations were prepared, and batch experiments were performed for the adsorption of Ni²⁺ ions present in the aqueous solution using fly ash (FA) and cow dung ash (CDA). During the batch experiments, the concentration of nickel ions was analysed using an atomic absorption spectrophotometer (GBC 932 AA). An oxidizing flame with air-acetylene was employed, and the measurements were conducted at a wavelength of 372.0 nm with a slit width of 0.2 nm. The chemical composition of the fly ash and cow dung ash was determined by conducting an XRF analysis using the Shimadzu EDX 7000 Series Energy Dispersive X-ray

Fluorescence Spectrometer.

The fly ash and cow dung particles were examined and studied by capturing magnified images using a Scanning Electronic Microscope (SEM 515, Philips).

Adsorbents

Fly ash, a fine powder waste was collected from a Bituminous coal-fired power station located in Nagpur, India. This fly ash was utilized as an adsorbent without any pre-treatment. The cow dung which is again a waste material was collected from a local Indian cow. The cow dung was sun-dried for 15 days and burned in the open area and the ash produced in such a way was used as an adsorbent without any further treatment. The major chemical constituents of fly ash (FA) and cow dung ash (CDA) are tabulated in Table 1.

The major chemical constituents of fly ash used are silica (65.01 %), alumina (24.41 %), and iron oxide (4.04 %). However, the main constituents of cow dung ash are silica (22.87 %), iron oxide (5.43 %), and lime (39.13 %) which makes it a class F fly ash as per ASTM [9]. Class F is low in lime, and contains a greater combination of silica, alumina, and iron (greater than 70 %). However, the cow dung ash is classified as Class C which contains about 39.13 % of CaO. To analyse the size distribution, the Indian Standard code [10] was used, and it was observed that for cow dung ash and fly ash, 99.1 % and 92 % of particles had a size less than 75 µm. Fig. 1 indicates the magnified image of fly ash particles and was observed that the fly ash particles are mostly spherical in nature. However, for the cow dung ash particles magnified image (Fig. 2) displays the microstructure of CaO-rich cow dung ash and shows a compact structure with a rough surface.

Kinetic models

It is very important to determine the rate law to study the sorption kinetics [11]. Five well-known kinetic models - pseudo - first order, pseudo - second order model, intra-particle diffusion model, Fractional power

Table 1. Chemical composition of fly ash (FA) and cow dung ash (CDA), %.

	SiO ₂	Al ₂ O ₃	Fe ₂ O ₃	CaO	TiO ₂	MgO	Na ₂ O	K ₂ O	P ₂ O ₅	SO ₃
FA	65.01	24.41	4.04	0.35	0.69	0.55	0.22	0.21	0.037	0.15
CDA	22.87	-	5.43	39.13	0.69	-	-	13.49	11.04	2.10

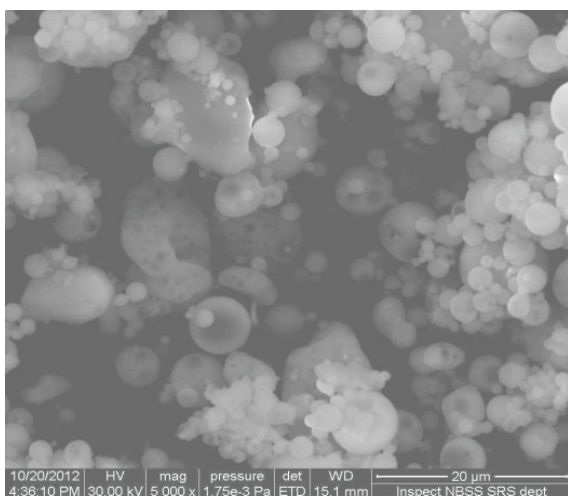


Fig. 1. SEM image of fly ash particles.

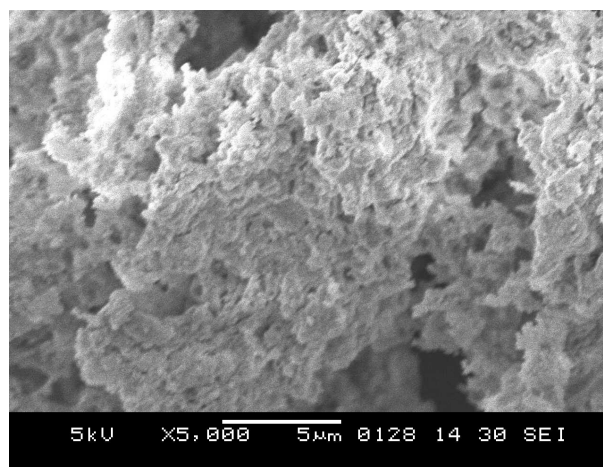


Fig. 2. SEM image of cow dung ash particles.

Table 2. Equations of different kinetic models used.

S. No.	Name of kinetic model	Expression	Kinetics constants	Plot
1	Pseudo-First Order [12]	$\ln(q_e - q_t) = \ln q_e - k_1 t$	q_e, k_1	$\ln(q_e - q_t)$ vs. t
2	Pseudo-Second Order [13]	$\frac{t}{q_t} = \frac{1}{k_2 q_e^2} + \frac{1}{q_e} t$	q_e, k_2	t/q_t vs. t
3	The Intra-particle Diffusion [14]	$q_t = K_{id} * t^{1/2} + C$	C, k_{id}	q_t vs. $t^{1/2}$
4	Fractional power [15]	$\ln q_t = \ln a + b \ln t$	a, b	$\ln q_t$ vs. $\ln t$
5	Elovich [16]	$q_t = \frac{1}{\beta} \ln(\alpha \beta) + \frac{1}{\beta} \ln t$	α, β	q_t vs. $\ln t$

model, and Elovich model were employed to describe the kinetic process. The mathematical equations, kinetic constants, and plot parameters of these five kinetic models are indicated in Table 2.

Error metrics

Having discussed different kinetic models for estimating the kinetic process, the main challenge is determining which kinetic model should be selected for describing the kinetic process of adsorption for fly ash and cow dung ash particles. In this regard, this paper has contributed an extensive evaluation for comparing and analysing the performance of different kinetic models. To achieve this, a total of eighteen

different error functions have been used that signify the performance of different models - how accurately a model is estimating the kinetic process. The details of these error functions are discussed in Table 3. For each error function, it can now be determined which kinetic model performs the best in terms of an accurate description of the kinetic process. Later, in Section Error analysis (Results and discussion), an additional error function Overall Performance Indicator is discussed that describes how to summarize the performance of different kinetic models with respect to different error function values obtained. This exhaustive evaluation and comparison are very significant in selecting the best-performing kinetic model.

Table 3. Details of error functions.

Sr. no.	Error function name	Abbreviation	Error function (y_t denotes true value of y, and y_p denotes predicted value of y)	Range and preferred value
1	Explained Variance Score [17]	EVS	$EVS(y_t, y_p) = 1 - \frac{\{Var\{y_t - y_p\}\}}{Var\{y_t\}}$	Bigger is better (Best = 1), Range = (-inf, 1.0]
2	Mean Bias Error [18]	MBE	$MBE(y_t, y_p) = \frac{1}{n} \sum_{i=1}^n (y_p^i - y_t^i)$	Best = 0, Range = (-inf, +inf)
3	Mean Squared Error [19]	MSE	$MSE(y_t, y_p) = \frac{\sum_{i=0}^{N-1} (y_t^i - y_p^i)^2}{N}$	Smaller is better (Best = 0), Range = [0, +inf)
4	Mean Squared Log Error [20]	MSLE	$MSLE(y_t, y_p) = \frac{1}{N} \sum_{i=0}^{N-1} \left((1 + y_t^i) - (1 + y_p^i) \right)^2$	Smaller is better (Best = 0), Range = [0, +inf)
5	Mean Relative Error / Mean Relative Bias [21]	MRE / MRB	$MRE(y_t, y_p) = \frac{1}{N} \sum_{i=0}^{N-1} \frac{ y_t^i - y_p^i }{ y_t^i }$	Smaller is better (Best = 0), Range = [0, +inf)
6	Mean Absolute Percentage Error [22]	MAPE	$MAPE(y_t, y_p) = \frac{1}{N} \sum_{i=0}^{N-1} \frac{ y_t^i - y_p^i }{ y_t^i } \times 100$	Smaller is better (Best = 0), Range = [0, +inf)
7	Mean Arctangent Absolute Percentage Error [23]	MAAPE	$MAAPE = \frac{100}{N} \sum_{i=1}^N \left \frac{y_t^i - y_p^i}{y_t^i} \right \arctan \arctan \left(\frac{y_t^i - y_p^i}{y_t^i} \right)$	Smaller is better (Best = 0), Range = [0, +inf)
8	Nash-Sutcliffe Efficiency Coefficient [24]	NSE	$NSE(y_t, y_p) = 1 - \frac{\sum_{i=0}^{N-1} (y_t^i - y_p^i)^2}{\sum_{i=0}^{N-1} (y_t^i - mean(y_t))^2}$	Bigger is better (Best = 1), Range = (-inf, 1]
9	Willmott Index [25]	WI	$WI(y_t, y_p) = 1 - \frac{\sum_{i=0}^{N-1} (y_t^i - y_p^i)^2}{\sum_{i=0}^{N-1} (y_p^i - mean(y_t) + y_t^i - mean(y_t))^2}$	Bigger is better (Best = 1), Range = [0, 1]
10	Absolute Pearson's Correlation Coefficient [26]	AR	$AR(y_t, y_p) = \frac{\sum_{i=0}^{N-1} (y_t^i - mean(y_t) \times y_p^i - mean(y_t))}{\sqrt{\sum_{i=0}^{N-1} (y_t^i - mean(y_t))^2} \times \sqrt{\sum_{i=0}^{N-1} (y_p^i - mean(y_t))^2}}$	Bigger is better (Best = 1), Range = [-1, 1]
11	Coefficient of Determination [27]	R^2	$R^2(y_t, y_p) = 1 - \frac{\sum_{i=1}^N (y_t^i - y_p^i)^2}{\sum_{i=1}^N (y_t^i - mean(y_t))^2}$	Bigger is better (Best = 1), Range = (-inf, 1]
12	Confidence Index [28]	CI	$CI(y_t, y_p) = AR(y_t, y_p) \times WI(y_t, y_p)$	Bigger is better (Best = 1), Range = (-inf, 1]

Table 3. Details of error functions - *continued*.

Sr. no.	Error function name	Abbreviation	Error function (y_t denotes true value of y , and y_p denotes predicted value of y)	Range and preferred value
13	Cross Entropy [29]	CE	$CE(y_t, y_p) = -\frac{1}{N} \sum_{i=1}^N [y_t^i \log \log (y_p^i) + (1 - y_t^i) \log \log (1 - y_p^i)]$	Range(-inf, 0], Can't give comment about this
14	Jensen Shannon Divergence [30]	JSD	$JSD(P Q) = \frac{1}{2} (KL(P M) + KL(Q M))$ where $M = \frac{1}{2}(P + Q)$, and KL is KL divergence.	Smaller is better (Best = 0), Range = [0, +inf)
15	Relative Absolute Error [31]	RAE	$RAE(y_t, y_p) = \frac{\sqrt{\sum_{i=1}^N (y_p^i - y_t^i)^2}}{\sqrt{\sum_{i=1}^N (y_t^i)^2}}$	Smaller is better (Best = 0), Range = [0, +inf)
16	Normalized Root Mean Square Error [32]	NRMSE	$NRMSE(y_t, y_p) = \frac{RMSE(y_t, y_p)}{mean(y_t)}$	Smaller is better (Best = 0), Range = [0, +inf)
17	Covariance [33]	COV	$COV(y_t, y_p) = \frac{\sum_{i=1}^N (y_t^i - mean(y_t))(y_p^i - mean(y_p))}{N - 1}$	Bigger is better (No best value), Range = (-inf, +inf)
18	Efficiency Coefficient [34]	EC	$EC(y_t, y_p) = 1 - \frac{\sum_{i=1}^N (y_t, y_p)^2}{\sum_{i=1}^N (y_t^i - mean(y_t))^2}$	Bigger is better (Best = 1), Range = (-inf, +1]

RESULTS AND DISCUSSION

Effect of contact time

The batch experiments to investigate the effect of contact time on adsorption under constant stirring conditions (150 rpm) were performed on the aqueous solution of Ni^{2+} ions. The stirring time was varied from 5 min to 180 min to achieve the equilibrium state. The adsorbent was separated from the solution by centrifuge at a speed of 3000 rpm for 5 min and the supernant Ni^{2+} solution was used to determine Ni^{2+} ions present in this solution, using atomic adsorption spectra.

The value of q_t was determined up to 3 h at different interval of time and the data is as plotted in Fig. 3 and it is concluded that initial adsorption is very high for FA and CDA but total adsorption is very high for CDA as compared to FA. The curves for FA and CDA become

relatively flat at about 180 min of adsorption, suggesting an equilibrium time of 3 h for the adsorption of nickel ions on FA and CDA. At equilibrium time, the value of q_e is determined as 0.089 $mg\ g^{-1}$ and 1.95 $mg\ g^{-1}$ for FA and CDA respectively.

Kinetics study

To study the different kinetic models the graphs are plotted and are as shown in Fig. 4 to Fig. 8. The various model constants are calculated from the linear equation obtained from the plot and tabulated in Table 4.

Error analysis

To analyse the suitability of different kinetic models, the value of q_t obtained from the different kinetic model equations are shown in Table 5. To identify the most accurate model for estimating q_t for cow dung and fly ash

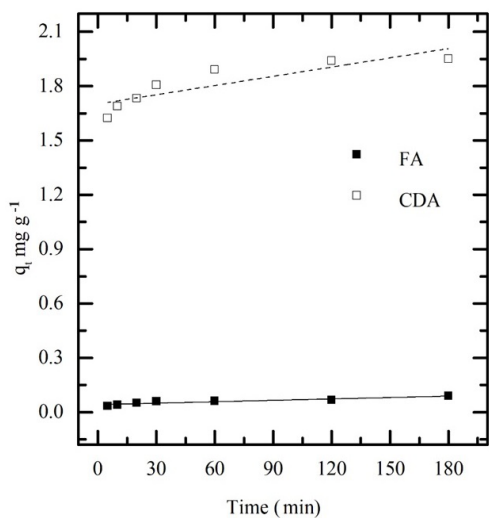


Fig. 3. Effect of contact time on q_t .

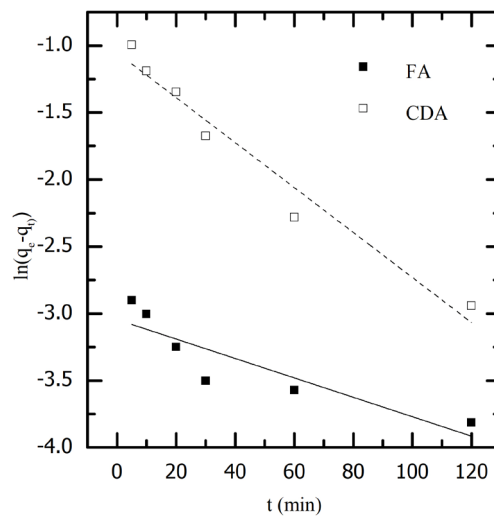


Fig. 4. The plot of pseudo-first order kinetics.

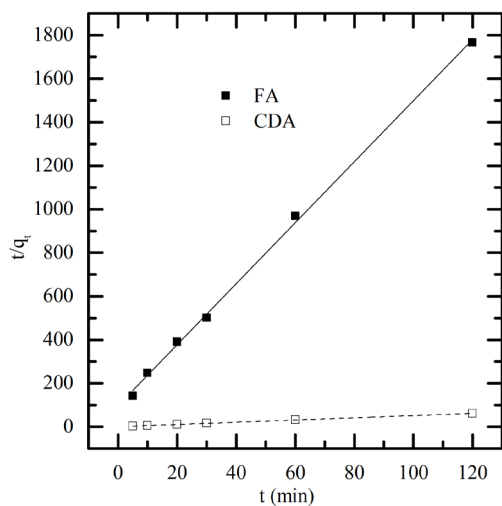


Fig. 5. The plot of pseudo-second order kinetics.

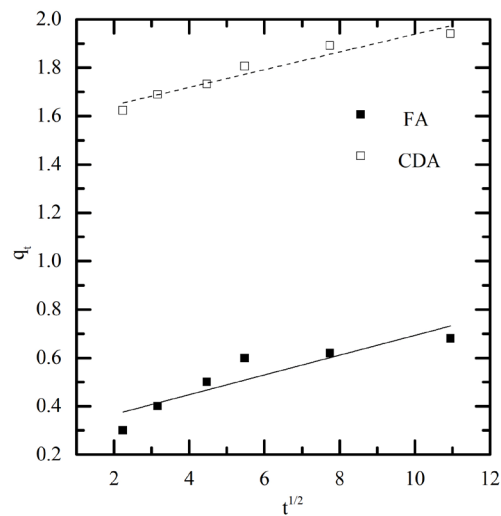


Fig. 6. The plot of intra-particle diffusion model.

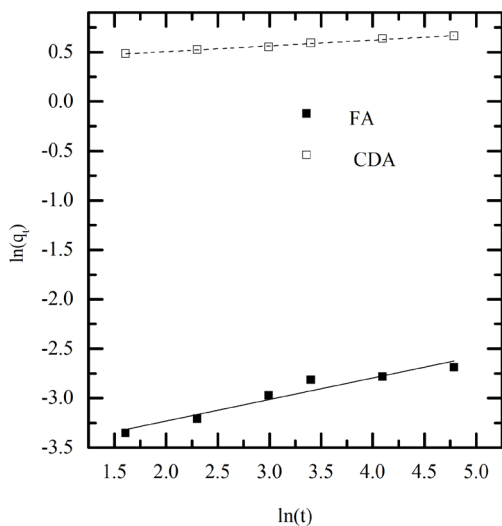


Fig. 7. The plot of Fractional Power model.

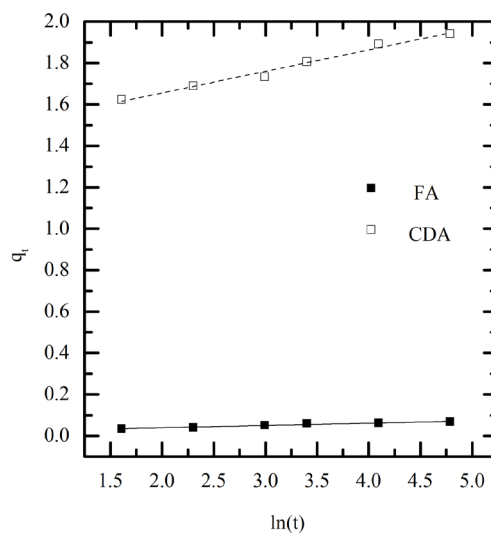


Fig. 8. The plot of Elovich model.

Table 4. Adsorption kinetics constants for various kinetic models.

Pseudo-first order kinetic model		
Model constants	k_1	q_e
FA	0.007	0.0476
CDA	0.017	0.3488
Pseudo-second order kinetic model		
Model constants	k_2	q_e
FA	2.0216	0.0714
CDA	0.2528	1.9666
Intra-particle diffusion model		
Model constants	K_{id}	C
FA	0.003	0.0317
CDA	0.0366	1.5727
Fractional power model		
Model constants	a	b
FA	0.031905	0.135
CDA	1.564	0.0364
Elovich model		
Model constants	α	β
FA	0.638061	166.66667
CDA	1743233342	15.45595054

adsorbent, a total of eighteen error functions (detailed in Table 3) have been discussed and used for the evaluation and comparison of different kinetic models. The values of these error functions for determining q_t using different kinetic models' particles is presented in Table 6 and Table 7 for cow dung and fly ash respectively. Based on preferred values of respective error functions mentioned in Table 3, the best performing model for each error metric is determined and highlighted in grey.

However, it may be observed that there is not one kinetic model that always performs the best with respect to all the error functions. Therefore, to address this issue of determining the overall best model, an error metric Overall Performance Indicator has been used (added at the end of Table 6 and Table 7) to summarize the performance of all the kinetic models in estimating q_t with respect to different error function values. It denotes the total number of times a particular kinetic model outperformed the remaining kinetic models with respect to a particular error metric under consideration. This is useful since some kinetic models may perform the best for some error metrics, while others may outperform this model. Therefore, this overall performance indicator is

Table 5. Value of q_t from the various kinetic model equation.

S. No.	Name of kinetic model	Time, t, min	For FA	For CDA
1	Pseudo-first order	5	0.0431	1.629
		10	0.0447	1.655
		20	0.0478	1.701
		30	0.0506	1.739
		60	0.0581	1.823
		120	0.0689	1.904
2	Pseudo-second order	5	0.0299	1.402
		10	0.0422	1.637
		20	0.0530	1.787
		30	0.0580	1.843
		60	0.0640	1.903
		120	0.0674	1.934
3	The Intra-particle diffusion	5	0.040	1.581
		10	0.043	1.584
		20	0.048	1.589
		30	0.052	1.593
		60	0.060	1.601
		120	0.072	1.613

Table 5. Value of q_t from the various kinetic model equation - *continued*.

S. No.	Name of kinetic model	Time, t, min	For FA	For CDA
4	Fractional power	5	0.035	1.605
		10	0.037	1.623
		20	0.038	1.641
		30	0.039	1.651
		60	0.041	1.669
		120	0.042	1.688
5	Elovich	5	0.034	1.599
		10	0.036	1.619
		20	0.038	1.638
		30	0.039	1.649
		60	0.041	1.669
		120	0.043	1.688

Table 6. Error function values for cow dung ash particles.

S. No.	Error functions	Kinetic models				
		Pseudo-first order	Pseudo-second order	The intra-particle diffusion	Fractional power	Elovich
1	Explained variance score	0.94955	0.31012	0.17966	0.43076	0.45897
2	Mean bias error	-0.03863	-0.0295	-0.18697	-0.1343	-0.1368
3	Mean squared error	0.00211	0.00936	0.04505	0.02504	0.02537
4	Mean squared log error	0.00027	0.00145	0.00602	0.00325	0.0033
5	Mean relative error / Mean relative bias	0.02235	0.03808	0.1019	0.0728	0.07428
6	Mean absolute percentage error	0.02235	0.03808	0.1019	0.0728	0.07428
7	Mean arctangent absolute percentage error	0.02234	0.03794	0.1013	0.07254	0.07402
8	Nash-Sutcliffe efficiency coefficient	0.82825	0.23956	-2.66129	-1.03509	-1.06196
9	Willmott index	0.95247	0.88893	0.4637	0.56413	0.56814
10	Absolute Pearson's correlation coefficient	0.98408	0.94742	0.97261	0.99146	0.99242
11	Coefficient of determination	0.82825	0.23956	-2.66129	-1.03509	-1.06196
12	Confidence Index	0.9783	0.98345	0.89499	0.92457	0.92317
13	Cross entropy	0.33952	0.28201	1.73378	1.22482	1.24734
14	Jensen Shannon divergence	94.9551	31.0125	17.96646	43.07561	45.8967
15	Relative absolute error	1	0.83333	0.5	0.66667	0.66667
16	Normalized root mean square error	0.07962	0.16754	0.36763	0.27408	0.27589

Table 6. Error function values for cow dung ash particles - *continued*.

S. No.	Error functions	Kinetic models				
		Pseudo-first order	Pseudo-second order	The intra-particle diffusion	Fractional power	Elovich
17	Covariance	0.98181	0.91926	0.96906	0.99146	0.99242
18	Efficiency coefficient	0.84166	0.4673	-1.16521	-0.26698	-0.28206
	Absolute overall performance indicator	11	3	2	0	2
	Percentage overall performance indicator	61	16.67	11.11	0	11.11

Table 7. Error function values for fly ash particles.

S. No.	Error functions	Kinetic models				
		Pseudo-first order	Pseudo-second order	The intra-particle diffusion	Fractional power	Elovich
1	Explained variance score	0.76631	0.95191	0.85229	0.34536	0.42955
2	Mean bias error	-0.00053	-0.00032	-0.00023	-0.01407	-0.01423
3	Mean squared error	3.00E-05	1.00E-05	2.00E-05	0.00029	0.00028
4	Mean squared log error	3.00E-05	1.00E-05	2.00E-05	0.00026	0.00026
5	Mean relative error / Mean relative bias	0.10569	0.04998	0.08185	0.23515	0.24158
6	Mean absolute percentage error	0.10569	0.04998	0.08185	0.23515	0.24158
7	Mean arctangent absolute percentage error	0.10472	0.0498	0.08153	0.22714	0.23383
8	Nash-Sutcliffe efficiency coefficient	0.76427	0.95119	0.8519	-1.07241	-1.02201
9	Willmott Index	0.92076	0.98877	0.95837	0.55039	0.57002
10	Absolute Pearson's correlation coefficient	0.92173	0.98398	0.93256	0.96525	0.97609
11	Coefficient of determination	0.76427	0.95119	0.8519	-1.07241	-1.02201
12	Confidence Index	0.98989	0.99399	0.99558	0.73325	0.73009
13	Cross entropy	0.00762	0.00354	0.00379	0.14829	0.14904
14	Jensen Shannon divergence	76.63066	95.19123	85.22877	34.53574	42.95472
15	Relative absolute error	0.66667	0.83333	0.66667	0.33333	0.16667
16	Normalized root mean square error	0.00993	0.00452	0.00787	0.02946	0.0291
17	Covariance	0.88535	0.98202	0.92322	0.96525	0.97609
18	Efficiency coefficient	0.79523	0.93605	0.85706	-0.29388	-0.26554
	Absolute overall performance indicator	0	14	2	1	1
	Percentage overall performance indicator	0	78	11	5.5	5.5

useful since it determines the kinetic model that should be selected based on these different error metrics. The performance indicator value is presented in absolute and percentage terms. Higher the value of overall performance indicator, the higher the accuracy of the kinetic model in estimating q_t .

It can be observed that for cow dung, the performance indicator metric is the highest for pseudo-first order kinetic model. This is because it outperforms the other models 11 times out of 18 error metrics, i.e. 61 %. However, the next best performing model is pseudo-second order kinetic model that has the best error metric value 3 times (16.67 %). But this is very low as compared to pseudo-first-order model. The intra particle diffusion and Elovich model perform the best two times each. But fractional power model never gives the best result for any error metric. Therefore, it can be concluded that for estimating q_t for cow dung ash, pseudo-first-order kinetic model should be preferred.

With respect to q_t determination for fly ash, pseudo-second order model performs the best 78 % of time (14 number in total). But the second best performing model is intra particle diffusion, which has the overall performance indicator score of only 11 % (2 times in total). Whereas fractional power and Elovich models perform the best 5.5 % number of times. However, here pseudo-first-order model doesn't perform the best for any error metric. This is interesting since pseudo-first order model performs the best for q_t determination for cow dung ash, but the same model does not give the best results for fly ash. These results show the dominance of pseudo-second order model over all kinetic models and should thus be chosen for fly ash q_t determination.

It can therefore be concluded that depending on the morphological properties of the adsorbent, different kinetic models may give the best approximation of q_t .

CONCLUSIONS

- The performance indicator indicates that for q_t estimation of cow dung ash, the ranking of kinetic models from best to worst is as follows: pseudo-first order (61 %), pseudo-second order (16.67 %), intra-particle diffusion (11.11 %), Elovich (11.11 %) and fractional power (0 %).

- Similarly, for fly ash adsorbent, the ranking of kinetic models from best to worst is: pseudo-second order

(78 %), intra-diffusion particle (11 %), fractional power (5.5 %), Elovich (5.5 %) and pseudo-first order (0 %).

- These results lead to an interesting observation that the pseudo-first order model performs the best q_t determination for cow dung ash, whereas the same model does not perform the best estimation of q_t for fly ash adsorbent.

- It can therefore be concluded that depending on the morphological properties of the adsorbent, different kinetic models may give the best approximation of q_t .

Authors contribution: *Ajay Kumar Agarwal, affirm that this research paper is the result of my independent work. The content, including ideas, analysis, and conclusions, reflects my own efforts and understanding of the topic. This statement serves as a declaration of my authorship and commitment to upholding scholarly standards.*

REFERENCES

1. A. González, N. Moreno, R. Navia, X. Querol, Development of a non-conventional sorbent from fly ash and its potential use in acid wastewater neutralization and heavy metal removal, *Chem. Eng. J.*, 166, 3, 2011, 896-905.
2. A.K. Saha, S. Choudhury, M. Majumder, Performance efficiency analysis of water treatment plants by using mcdm and neural network model, *Matter: Int. J. Sci. Tech.*, 3, 1, 2017, 27-35.
3. S.M. Kanawade, R.W. Gaikwad, Removal of Dyes from Dye Effluent by Using Sugarcane Bagasse Ash as an Adsorbent, *Int. J. Chem. Eng. Appl.*, 2, 2011, 202-206.
4. I.L. Muthreja, A.K. Agarwal, M.S. Kadu, C.P. Pandhurnekar, Adsorption and Kinetic Behavior of Fly Ash Used for the Removal of Lead from an Aqueous Solution, *J. Chem. Technol. Metall.*, 52, 3, 2017, 505 - 512.
5. J.T. Matheickal, M.Y. Qi, Biosorption of lead from aqueous solutions by marine algae eckloniaradiata, *Wat. Sci. Tech.*, 34, 9, 1996, 1-7.
6. A. Radjenovic, G. Medunic, Adsorptive Removal of Cr(VI) from Aqueous Solution by Carbon Black, *J. Chem. Technol. Metall.*, 50, 1, 2015, 81-88.
7. W.J. Weber, Adsorption Theory, Concepts and Models, *Adsorption Technology: A Step by Step Approach to Process Evaluation and Application*,

- Marcel Dekker, New York, 1985.
8. C.H. Chakrapani, C.H. Suresh Babu, K.N.K. Vani, K. Somasekhara Rao, Adsorption Kinetics for the Removal of Fluoride from Aqueous Solution by Activated Carbon Adsorbents Derived from the Peels of Selected Citrus Fruits, *J. Chem.*, 7, S1, 2010, S419-S427.
 9. A.R. Pourkhorshidi, M. Najimi, T. Parhizkar, F. Jafarpour, B. Hillemeier, Applicability of the standard specifications of ASTM C618 for evaluation of natural pozzolans, *Cem. Concr. Compos.*, 32, 10, 2010, 794-800.
 10. Indian Standard Code, IS 2720: 1985, Methods of test for soils.
 11. M.N. Rashed, A.A. G. Arfeen, F.A. El-Dowy, Removal of Rhodamine-B dye using chemically modified activated Muscovite: kinetics, isotherms, and thermodynamic studies, *J. Chem. Technol. Metall.*, 58, 1, 2023, 143-152.
 12. P.C. Mishra, R.K. Patel, Removal of nickel and zinc ions from water by low-cost adsorbents, *J. Haz. Matter.*, 168, 2009, 319-325.
 13. Y.S. Ho, G. McKay, The kinetics of sorption of divalent metal ions onto sphagnum moss peat, *Water Res.*, 34, 3, 2000, 735-742.
 14. W.J. Weber, J.C. Morris, Kinetics of adsorption on carbon from solution, *J. Sanit. Eng. Div., ASCE*, 89, 1963, 31-60.
 15. R.C. Dalal, Desorption of soil phosphate by anion exchange resin, *Commun. Soil Sci. Plant Anal.*, 5, 6, 1974, 531-538.
 16. M. Avrami, Kinetics of phase change I general theory, *J. Chem. Phys.*, 7, 1939, 1103-1112.
 17. T. Nguyen, G. Nguyen, B.M. Nguyen, Eo-cnn: an enhanced cnn model trained by equilibrium optimization for traffic transportation prediction, *Procedia Computer Science*, 176, 2020, 800-809.
 18. K. Takeyoshi, Prediction of photovoltaic power generation output and network operation, *Integration of Distributed Energy Resources in Power Systems*, Academic Press, 2016, 77-108.
 19. K. Das, J. Jiang, J.N.K. Rao, Mean Squared Error of Empirical Predictor, *Ann. Stat.*, 32, 2, 2004, 818-840.
 20. T.O. Hodson, M.O. Thomas, S.F. Sydney, Mean squared error, deconstructed, *J. Adv. Model. Earth Syst.*, 13, 12, 2021, 1-10.
 21. S. Jain, P.K. Mishra, V.V. Thakare, J. Mishra, Design of microstrip moisture sensor for determination of moisture content in rice with improved mean relative error, *Microw. Opt. Technol. Lett.*, 61, 7, 2019, 1764-1768.
 22. T. Nguyen, B. Hoang, G. Nguyen, B. M. Nguyen, A new workload prediction model using extreme learning machine and enhanced tug of war optimization, *Procedia Computer Science*, 170, 2020, 362-369.
 23. R. Liu, T. Chen, G. Sun, S. M. Muyeen, S. Lin, Y. Mi, Short-term probabilistic building load forecasting based on feature integrated artificial intelligent approach, *Electr. Power Syst. Res.*, 206, 2022, 107802.
 24. C. Xie, H. Nguyen, X. N. Bui, V. Nguyen, J. Zhou, Predicting roof displacement of roadways in underground coal mines using adaptive neuro-fuzzy inference system optimized by various physics-based optimization algorithms, *J. Rock Mech. Geotech. Eng.*, 13, 6, 2021, 452-1465.
 25. R.D. da Silva, M.A. de Aguiar, M.G. Canteri, J.R. Rosisca, N.A. Vieira Junio, Reference evapotranspiration for londrina, paran, brazil: performance of different estimation methods, *Semina: Cincias Agrrias*, 38, 4, 2017, 2363-2374.
 26. P. Schober, C. Boer, L.A. Schwarte, Correlation coefficients: appropriate use and interpretation, *Anesth. Analg.*, 126, 5, 2018, 1763-1768.
 27. B.M. Nguyen, B. Hoang, T. Nguyen, G. Nguyen, Nqsv-net: a novel queuing search variant for global space search and workload modelling, *J. Ambient Intell. Humaniz. Comput.*, 12, 2021, 27-46.
 28. A.N. Ahmed, T.V. Lam, D.H. Nguyen, V.T. Nguyen, K. Ozgur, A. El-Shafie, A comprehensive comparison of recent developed meta-heuristic algorithms for streamflow time series forecasting problem, *Appl. Soft Comput.*, 105, 2021, 107282.
 29. P.T. De Boer, D.P. Kroese, S. Mannor, R.Y. Rubinstein, A tutorial on the cross-entropy method, *Ann. Oper. Res.*, 134, 2005, 19-67.
 30. B. Fuglede, F. Topsøe, Jensen-Shannon divergence and hilbert space embedding, *International Symposium on Information theory, ISIT 2004. Proceedings IEEE*, 31, 2004.
 31. K. Chen, S. Guo, Y. Lin, Z. Ying, Least absolute relative error estimation, *J. Am. Stat. Assoc.*, 105, 491, 2010, 1104-1112.

32. K.D. Stephen, A. Kazemi, Improved normalization of time-lapse seismic data using normalized root mean square repeatability data to improve automatic production and seismic history matching in the nelson field, *Geophys. Prospect.*, 62, 5, 2014, 1009-1027.
33. A. R. Wildt, O. Ahtola, *Analysis of covariance*, Sage, 12, 1978.
34. K.G. Jöreskog, *Structural analysis of covariance and correlation matrices*, *Psychometrika*, 43, 4, 1978, 443-477.